



Mass Determination of Coronal Mass Ejection by Thomson Equations

M. A. M. Al OBAID^{a*}, A.A. SELMAN^b

^a Department of astronomy and space, College of Science, University of Baghdad, Baghdad, IRAQ.

^b Department of astronomy and space, College of Science, University of Baghdad, Baghdad, IRAQ.

Abstract:

One of the main sources of calculating the mass of coronal mass ejections (CME) is the use of Large Angle and Spectrometric Coronagraph (LASCO) detectors onboard Solar and Heliospheric Observatory (SOHO) images and using Thomson Scattering of white light from the outer edge of the CME plasma. Thomson Scattering of white light from the outer edge of the CME have also been used in set of equations in this paper, to describe light scattering from the outer edge of the CME. These equations depend on many functions, each of which is described by the angular dependence between the Sun-Earth line of sight. The angular parameters were calculated and then the final mass dependence on angle was numerically estimated using a MATLAB code. The results showed that a similar dependence of few functions on the angles and the distance of the CME outer edge from center of the Sun. A comparison was made for two distances, the conclusion was when that distance increases the mass distribution decreases.

Keywords: Thomson Scattering, Coronal Mass Ejection, Solar Corona.

DOI:

1. INTRODUCTION

Coronal Mass Ejection are observed in visible white light by coronagraphs which block out the light from the photosphere. This is made possible because CMEs are comprised of plasma, so they contain large numbers of free electrons. The observed white light is originally from the photosphere and is scattered off these electrons via a process called Thomson scattering.

In order to completely understand the evolution of CMEs, it is necessary to understand the meaning of changes in their appearance in coronagraph and heliospheric images. With careful analysis of the white light images and a detailed understanding of the Thomson scattering physics and projection geometry, it is possible to extract a great deal of information about the CME from their white light images.

This paper addresses the analysis surrounding how CMEs is observed in white light. Begin with the basics

of Thomson scattering theory and build up a picture of a CME from a line-of-sight integration to a volume of electrons. The first white light observations of the CME would occur during the 1970's and must have been a most beautiful and spectacular finding [1].

The objective is to identify how the appearance of a CME image changes due to the physics surrounding its appearance, particularly at large distances from the Sun [2].

The solar corona is not stable, but is constantly escaping into space. Although the magnetic field of the Sun, some of the hot gases near the solar surface to make spectacular prominences, in other regions the magnetic field opens into interplanetary space and allows the million-degree gases to escape as a solar wind [3].

CMEs are observed by coronagraphs, which block out the main body of light from the Sun to reveal the faint surrounding corona [4]. Huge ejections of plasma in the Sun's outer atmosphere can be detected by coronagraphs

and these ejections usually have speeds of a few tens of km/s up to more than 2000 km/s, an average outward propelled mass of ~ 1012 kg of solar material. CMEs can be observed by today's most sophisticated space borne white-light coronagraph Large Angle and Spectrometric Coronagraph (LASCO) on board SOHO [5].

2. DATA

This paper aims to study and calculate the mass content in Coronal Mass Ejection using available data from Large Angle and Spectrometric Coronagraph (LASCO) detectors onboard Solar and Heliospheric Observatory (SOHO) mission. MATLAB programs were used to achieve the objectives of this study.

3. THEORY

3.1. Methods of CME Study

CMEs are provided by imaging observations made in EUV, X-rays, H α and in radio [6]. The H α and other visible line emission on picture are due to heating of the chromosphere by conduction of the hot soft X-ray emitting plasma in the flare loop. While the occasional white-light emission, if at the temperature minimum, could be due to protons penetrating to this level. The solar atmosphere is best seen in H α because it occurs in the middle of the big dark H α absorption line. This absorption line falls in the red part of the visible spectrum and leads us to more understand the relation of the flare to the contact of the magnetic field, filaments, Sunspot and CME [7].

3.2. Distance Measurement Using LASCO Images

Howard suggested that all measurements made from coronagraph images are projected into the sky plane, as in Figure (1). In the case of LASCO, measured distances in solar radii are actually measurements of elongation ϵ , that is, the angle between the Sun-Earth line and the line from the Earth to the measured point P. Elongation is converted to distance with the application of two assumptions:

1. Light from P is Thomson scattered such that the line from the Earth to P is at right angles to the line from the Sun to P. This approximation can be expressed as ($R \sim \sin \epsilon$), where R is the distance from the Sun to P in units of AU.

2. Elongation angles are small, such that ($\sin \epsilon \sim \epsilon$), and hence ($R \sim \epsilon$).

Therefore for conversion of elongation angle to distance in solar radii, one simply takes ϵ in radians and multiplies by 1 AU in units of R_{\odot} , or $R \sim 216\epsilon$ [4].

3.3. Mass Determination by Thomson Equations

The determination of mass in the "CDAW SOHO LASCO Catalog" is based on the assumption that the mass of the CME is localized in the plane of the sky and that the integrated line of sight intensity is equal to the CME intensity at the point P being measured. LASCO CME mass is estimated using measurements of the brightness of the CME and the theory of Thomson scattering. Thomson-scattered white light from the Sun is maximized when the observer-P vector is orthogonal to the Sun-P vector (in the plane of the sky for a limb CME), and when this is not the case only a component of the scattered light at P is observed [4].

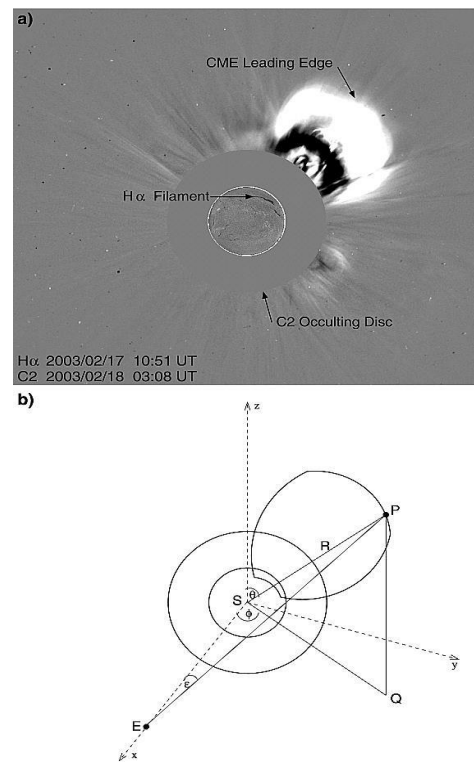


Figure 1: (a) LASCO, C2 image with a H α superimposed. (b) A schematic diagram of the image in (a) with the associated geometry overlaid [4].

For a sky plane assumption, $\theta = 0$ and $\sin \Omega = 1/R_0$. CME mass (m) is calculated by measuring the integrated intensity across a selected area on a running difference image β_{obs} .

$$\sin \Omega = \frac{\cos \theta}{R_0} \quad (3.1)$$

Where (θ) is the angle of the line SP to the plane of the sky.

Here, $B_e(\theta)$, known as the Thomson scattering function, is given by:

$$A(R) = \cos \Omega \sin^2 \Omega \quad (3.2)$$

$$B(R) =$$

$$-\frac{1}{8} \left[1 - 3 \sin^2 \Omega - \cos^2 \Omega \left(\frac{1+3\sin^2 \Omega}{\sin \Omega} \right) \ln \left(\frac{1+\sin \Omega}{\cos \Omega} \right) \right] \quad (3.3)$$

$$C(R) = \frac{4}{3} - \cos \Omega - \frac{\cos^2 \Omega}{3} \quad (3.4)$$

$$D(R) =$$

$$-\frac{1}{8} \left[5 + \sin^2 \Omega - \cos^2 \Omega \left(\frac{5-\sin^2 \Omega}{\sin \Omega} \right) \ln \left(\frac{1+\sin \Omega}{\cos \Omega} \right) \right] \quad (3.5)$$

$$B_e(\theta) =$$

$$\frac{\sigma \pi}{2} \left[2(C + u(D - C)) \cos^2 \theta (A + u(B - A)) \right] \quad (3.6)$$

$$m = \frac{B_{\text{obs}}}{B_e(\theta)} \times 1.97 \times 10^{-27} \text{ Kg} \quad (3.7)$$

Where σ is the scattering cross section, 7.95×10^{-26} per steradian and u accounts for limb darkening, $\mu = 0.63$. Mass measurements are therefore strongly dependent on angle θ but a direct relationship between $m(\theta)$ and $m(0)$ cannot be determined. To correct for projection in the mass measurements, it is necessary to repeat the measurements made for the catalog with the same value of B_{obs} but with θ equal to the direction of propagation of the CME. Without knowledge of the original value of B_{obs} .

4. RESULT and DISCUSSION

4.1. Results and Analyzed of Mass Determination by Thomson Equations

4.1.1. When $\epsilon=1$

In Figure (2) the results of the function $A(R)$ taken from equation (3.2). it is seen that the function reaches a maximum at $\theta = \pi/2$ and $\phi = 0$, while in Figure (3) the results of the function $B(R)$ taken from equation (3.3). In Figure (4), the equation (3.4) was calculated for the function $C(R)$, and in Figure (5) equation (3.5) was calculated for $D(R)$.

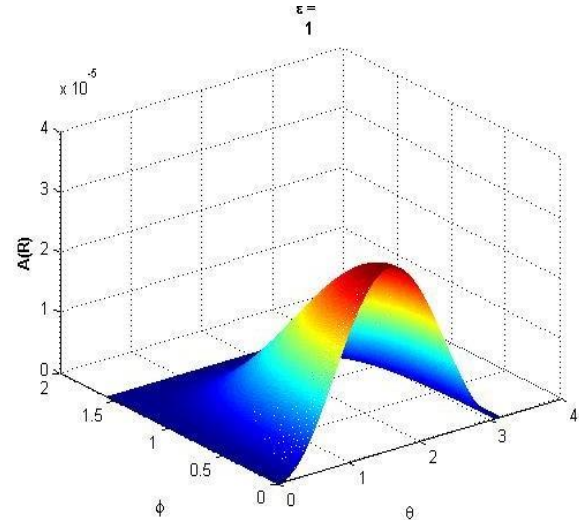


Figure 2: The result of function $A(R)$ at $\epsilon=1$

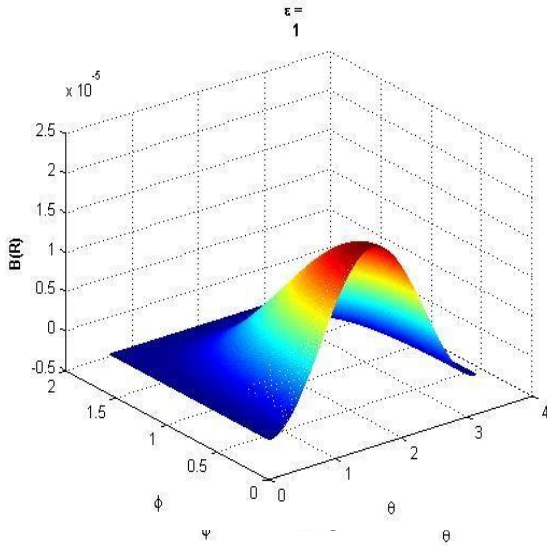


Figure 3: The result of function B(R) at $\varepsilon=1$

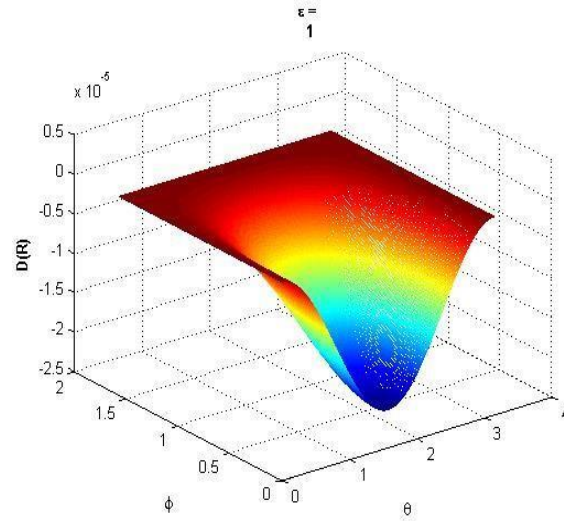


Figure 5: The result of function D(R) at $\varepsilon=1$

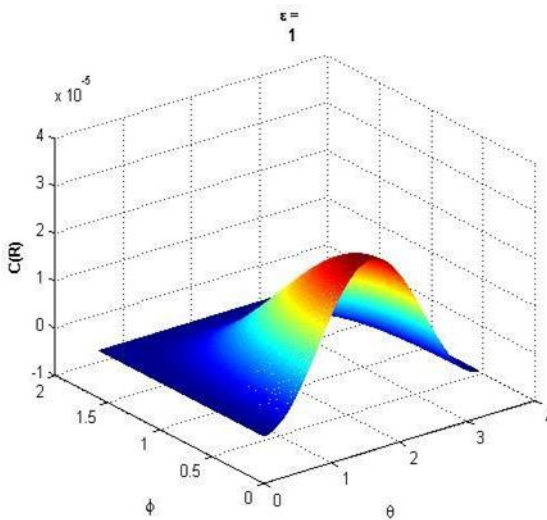


Figure 4: The result of function C(R) at $\varepsilon=1$

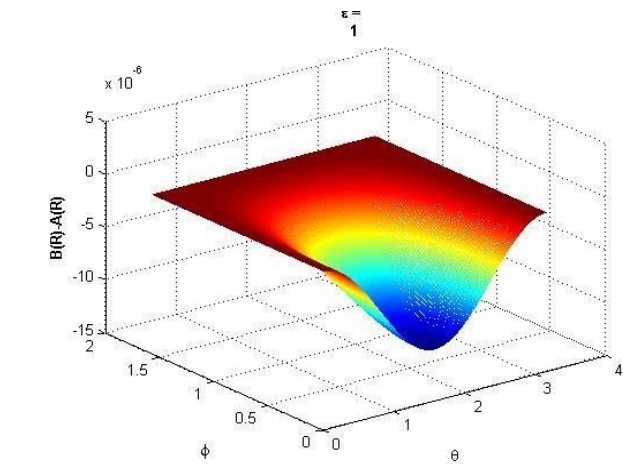


Figure 6: The result of function B(R)-A(R)

In Figure (6), the difference between B(R) and A(R) was plotted, while in Figure (7) the difference between C(R) and A(R) is shown. These two figures were made in order to show the small differences between these functions which were in general behaving similarly.

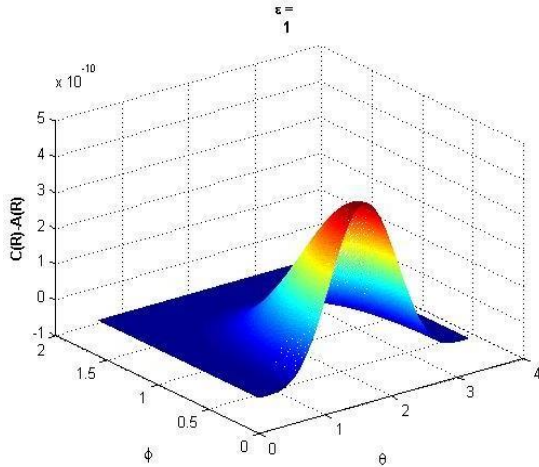


Figure 7: The result of function C(R)- A(R)

In Figure (8), the product of A(R) B(R) C(R) D(R) is shown in a two-dimensional plot. This is made in order to have a general insight of these functions when projected upon each other's. In Figure (9), the same result is shown in a 3-D plot.

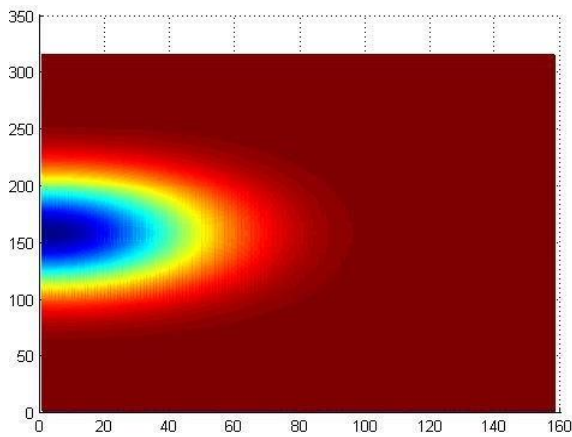


Figure 8: The 2-D result of multiplication of A.B.C.D

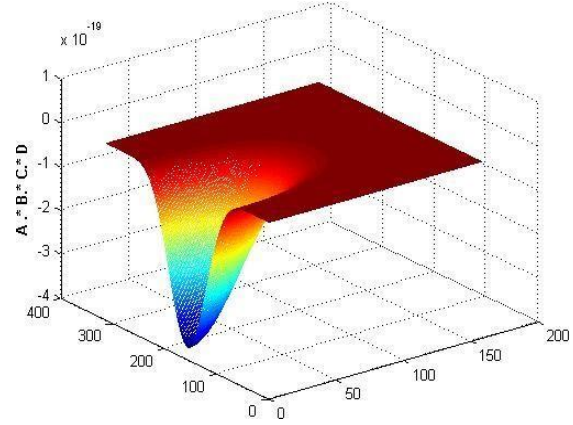


Figure 9: The result of multiplication of A.B.C.D in angle 3-D plot.

In Figure (10), the results of Thomson scattering, equation (3.6) is shown. We can see that the function behaves like Figure (2) of the function A(R) but with obvious difference in the z-scale. Also the peak is somewhat narrower than the function of A(R). Be uses all the previous functions, namely, A, B, C and D. Therefore it sums over all the important differences of these functions – hence we have calculated the multiplication of them in Figures (8) and (9). This important equation is used into equation (3.7) to calculate the mass of the CME. This is shown in Figure (11).

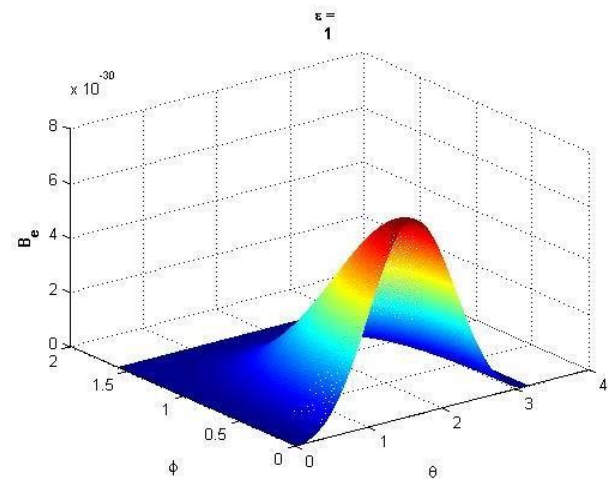


Figure 10: The result of function Be.

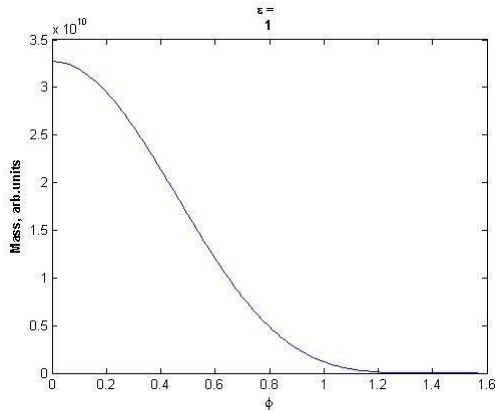


Figure 11: The result of mass calculation

The equation (3.6) uses Bobs, which is the difference between two success images from SOHO/LASCO C3 images. However, we could not complete this task because the program was too complicated. Thus we used a single image as input.

From Figure (11), we see that the mass decreases as the radial distance ϕ increases. The maximum is at $\phi=0$. At $\phi \sim 1.2$ radian, the mass value drops to zero. This is the region far away from the main body of the CME.

4.1.2. When $\epsilon=0.01$

The same equation were repeated for calculations at $\epsilon=0.01$.

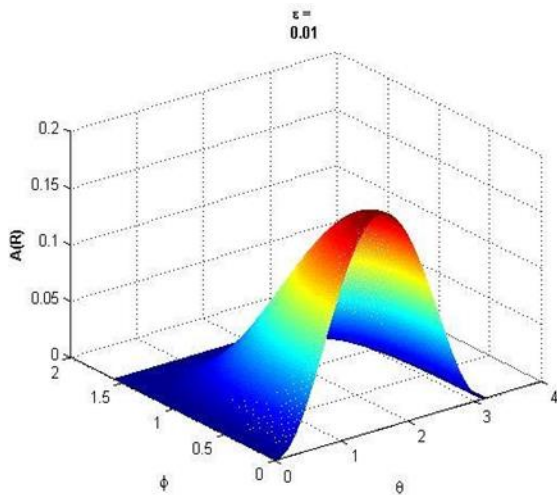


Figure 12: The result of function A(R) at $\epsilon=0.01$

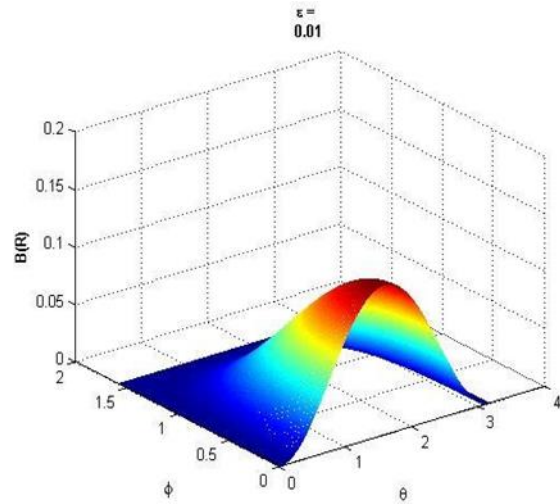


Figure 13: The result of function B(R) at $\epsilon=0.01$

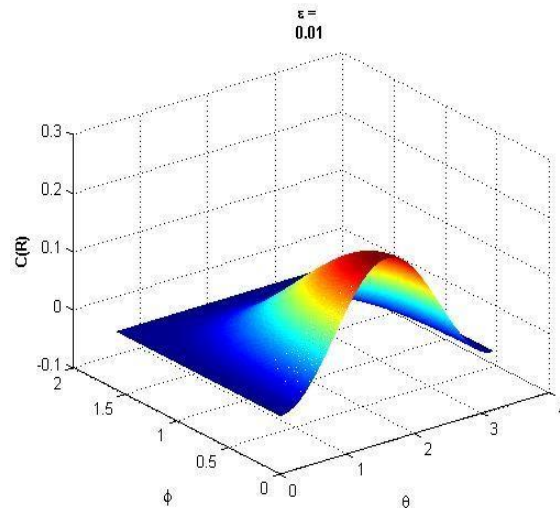


Figure 14: The result of function C(R) at $\epsilon=0.01$

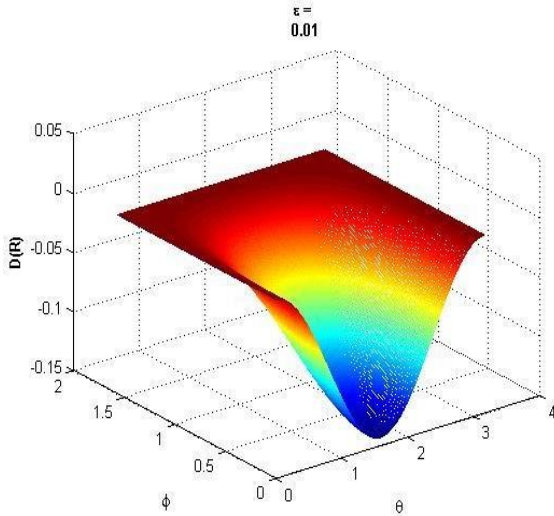


Figure 15: The result of function $D(R)$ at $\varepsilon = 0.01$

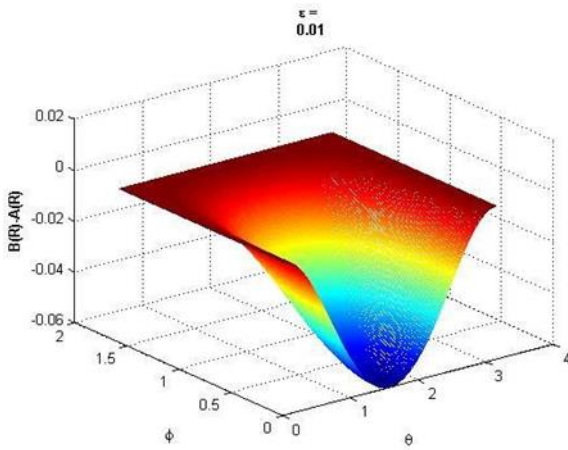


Figure 16: The result of function $B(R)-A(R)$ at $\varepsilon = 0.01$

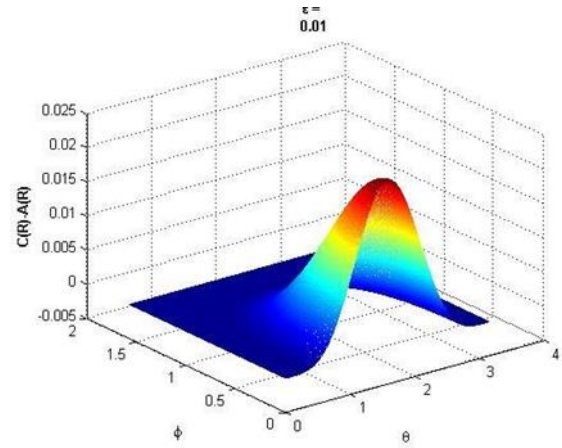


Figure 17: The result of function $C(R)-A(R)$ at $\varepsilon = 0.01$

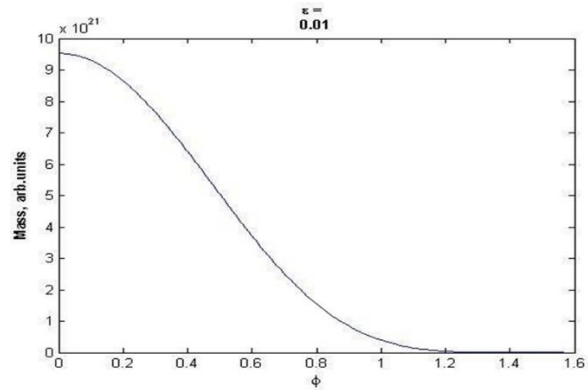


Figure 18: The mass result at $\varepsilon = 0.01$

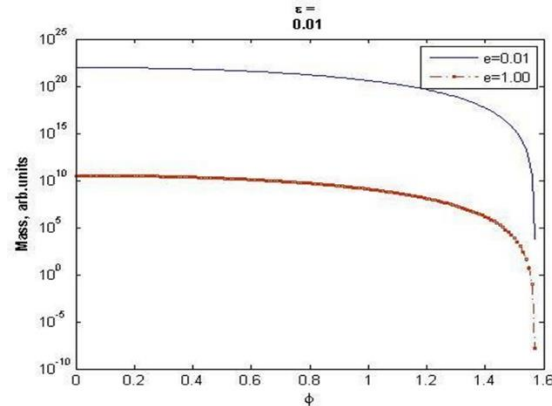


Figure 19: A comparison between mass calculations of $\varepsilon = 1$ and $\varepsilon = 0.01$



In Figure (19), a comparison was made between mass calculations at $\varepsilon=1$ and $\varepsilon=0.01$.

The result clearly shows that the mass at $\varepsilon=0.01$ difference is $\sim 10^{12}$ times larger the mass at $\varepsilon=1$. This clearly shows that CME masses near the sun have very large masses and as they move away into interstellar space the mass drops significantly.

5. FUTURE WORK

Developing a MATLAB code to fully investigate Thomson scattering for mass calculation.

6. REFERENCES

- [1]. Olmedo O., "A Study of the initiation process of Coronal Mass Ejections and the tool for their auto-detection" George Mason University, Spring Semester, 2011.
- [2]. Howard T., "Coronal Mass Ejections: An Introduction", Astrophysics and Space Science Library, Springer, vol.367, 2011
- [3]. Burch J., Taylor W., and Higley S., "Solar Storms and You! Exploring the Wind from the Sun" National Aeronautics and Space Administration, pp. 9-12, 2000.
- [4]. Howard T., Nandy N., and Koepke A. C., "Kinematic properties of solar coronal mass ejections: Correction for projection effects in spacecraft Coronagraph measurements" Journal of Geophysical Research, Vol. 113 (2008) A01104,.
- [5]. Bothmer V., "Solar corona, solar wind structure and solar particle events" Kiel, Kiel, Germany, 1999.
- [6]. Pick M., "Overview of Solar Radio Physics and Interplanetary Disturbances" Astrophysics and Space Science Library, Ch. 2, vol. 314, 2004, pp. 17-45.
- [7]. Philips, K.J.N., Cambridge University, 187 (1992) 195,196,224.